Highspeed Laser Micro Processing using Ultrashort Laser Pulses

Joerg SCHILLE [*1,2], Lutz SCHNEIDER[*1], Mathias MUELLER[*1], Udo LOESCHNER[*1], Nicholas GODDARD[*2], Patricia SCULLY[*2] and Horst EXNER[*1]

[*1] *University of Applied Sciences Mittweida, Technikumplatz 17, 09648 Mittweida, Germany.*
schille@hs-mittweida.de
[*2] *School of Chemical Engineering and Analytical Science, The University of Manchester, Oxford Road, Manchester, M13 9PL, United Kingdom.*

This paper discusses results obtained in highspeed laser micro processing of zirconium oxide ceramic and stainless steel. High-repetition rate femtosecond laser systems were joined together with fast galvanometer scan systems. Both, high average laser power (31.7 W) and fast scan speeds (17.1 m/s) were applied in order to increase material removal. The impact of average laser power, laser energy and repetition rate on both the volume ablation rate and the machining quality was studied. The maximum volume ablation rate for zirconium oxide was 70.3 µm³ per pulse, obtained with 5.9 µJ at 1.02 MHz. It is demonstrated that material removal on zirconium oxide will be strongly affected by heat. Stainless steel was irradiated with laser power up to 31.7 W and various repetition rates. The maximum material removal rate was found to be 6.8 mm³ / min, achieved with laser pulses of 0.85 J/cm² fluence. The feasibility of the highspeed laser technology in micro processing is verified by demonstrator structures. Finally, a laser processing rate of 25 cm² / min is demonstrated for a rectangular structure with the dimension of 80 x 80 mm².

Keywords: ultrashort, micro processing, micromachining, highspeed, stainless steel, zirconium oxide, heat accumulation, particle shielding, high-repetition rate, high PRF

1. Introduction

The unique advantages of ultrashort laser pulses in micro processing are high efficiency, fast and localized energy deposition, and minimal thermal load of the work piece. These benefits suggest initially a great potential of the ultrashort pulse laser technology in micromachining with respect to accuracy, precision and machining quality. Moreover, by using the recently developed high-repetition rate femtosecond laser technology, a great leap in terms of processing speed can be suggested to overcome the technological drawback of limited throughput.

However, little research has been done up to now using high-PRF (pulse repetition frequency) femtosecond laser systems in micro processing [1-7]. In these studies, heat accumulation and particle shielding have been identified as new interaction phenomena for ultrashort laser pulses, mainly caused by the short temporal distance between consecutive incident pulses. Thus a further impact of these phenomena on material removal must be expected by using higher laser power or/and higher repetition rates.

This paper presents results obtained in studying highspeed laser micro processing of zirconium oxide and stainless steel. High-repetition rate femtosecond laser systems with maximum laser power of 31.7 W were joined together with fast galvanometer scan systems. The laser beam was deflected with scan speeds up to 17.1 m/s in order to increase material removal. The impact of average laser power, laser energy and repetition rate on both the volume ablation rate and the machining quality is analyzed.

2. Fundamentals of high-PRF laser ablation

In recent studies investigating high-PRF laser processing, heat accumulation and particle shielding have been identified in laser matter interaction [1, 6, 7]. Accumulation of heat takes place particularly in low heat-conductive materials, such as stainless steel, because of the time between high-PRF laser pulses is too short for complete heat dissipation. Even for ultrashort laser pulses a significant fraction of absorbed laser energy will be deposited into the bulk closely around the surface of the processing area, causing surface temperature increase.

Figure 1 gives a schematic view on dissipation of heat, illustrated for five irradiated laser pulses on stainless steel. The heat affected volume is estimated based on the heat diffusion length $\mathbf{l_d}$. In the figure, different depths of heat propagation can be recognized depending on the repetition rate. This can be explained by the differing periods of time $\mathbf{\Delta t}$ between consecutive incident laser pulses.

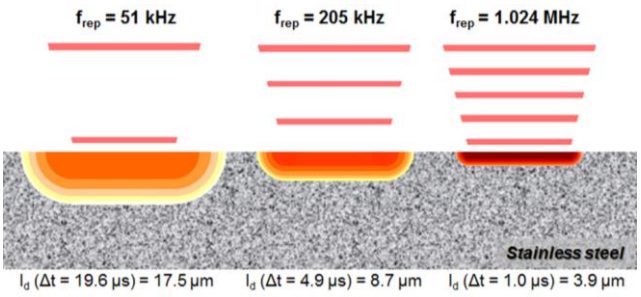

Figure 1: Heat affected volume illustrated for stainless steel and different repetition rates; heat diffusion lengths $\mathbf{l_d}$ are presented.

For the time between two incident laser pulses at 51 kHz, 205 kHz, and 1.02 MHz repetition rate, the heat diffusion lengths calculate to 17.5 µm, 8.7 µm, and 3.9 µm, respectively. As a result, a significant smaller area will be affected by heat at the highest investigated pulse repetition rate. Thus, by assuming that the amount of deposited laser energy is unaffected by the repetition rate, a much stronger surface temperature rise can be suggested for the smallest heat affected volume compared to the larger ones.

The impact of the pulse repetition rate on the surface temperature was assessed exemplarily on stainless steel. Enhanced energy coupling was suggested to estimate the amount of thermal energy deposited within the near-surface area with each irradiated laser pulse. This assumption is based on results achieved in direct observation of temperature fields during multiple femtosecond laser ablations. For steel it was reported that a significant high fraction of incident laser power up to 70% will be deposited into the solid as thermal energy [8].

Figure 2 presents results achieved in a simplified surface temperature calculation. The surface temperature rise for 100 consecutive irradiated laser pulses at different repetition rates is shown. In this calculation both the deposited thermal energy and the heat affected volume was taken into account. A thermal energy input of 3.5 µJ per irradiated laser pulse was considered. This is 70% of the irradiated laser pulse energy of 5 µJ.

In case of the lowest examined repetition rate of 51 kHz, the surface temperature increased slightly with increasing number of incident laser pulses. The maximum surface temperature was calculated of almost 100°C, obtained after 100 pulses. For the higher repetition rate of 205 kHz a temperature rise up to 390°C was calculated, which is considerably lower the melting temperature of stainless steel. The highest surface temperature of almost 1,800°C was obtained at the highest repetition rate of 1.02 MHz.

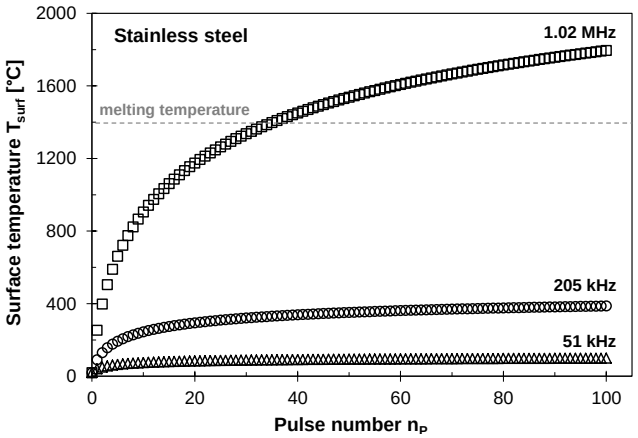

Figure 2: Surface temperature calculation on stainless steel, a thermal input of 3.5 µJ was taken into calculation, the repetition rate was varied between 51 kHz, 205 kHz and 1.02 MHz.

Further it can be seen from Figure 2 that the melting temperature of stainless steel will be exceeded after 30 incident laser pulses. This is due to the fact that thermal energy will be deposited in a small near-surface area as a result of both low heat conductivity and small temporal pulse-to-pulse distances. Moreover, this strong temperature increase will give rise to both higher laser beam absorption and lower ablation thresholds, causing more efficient material removal. On the other hand this study demonstrates that even ultrashort pulse laser ablation is a thermal process causing material melting to take place.

In high-PRF laser processing particle shielding has been identified as another significant material removal influencing effect. It has been shown already that metal removal rates decreased at pulse repetition rates above several hundred kilohertz [1]. This is due to the insufficient time for the ablation products to clear between the high-PRF laser pulses. As a result the next following laser pulses interact with ablated particles and droplets.

Supporting this, ablation plumes arising on stainless steel upon femtosecond laser irradiation are presented in Figure 3. A time range of 1 µs is recorded with an ultra speed intensified camera system (hsfc pro, PCO), correlating to the time base of laser pulses at 1 MHz repetition rate. The photographs give evidence that the ablation particle plume is still existent in times up to 1 µs. From this, it can be concluded that high-PRF laser pulses at repetition rates in the range of 1 MHz or higher will be scattered, reflected or/and absorbed by the remaining ablation products, causing partially shielding of the work piece.

Furthermore it can be seen in Figure 3 that the ablation plume enlarged at the higher repetition rates. For this, the increase of material removal can be suggested by using high-PRF laser pulses. This is conclusive to results presented in an earlier work [7]. It was demonstrated that particle shielding losses have been overbalanced by heat accumulation, enhancing the material removal process.

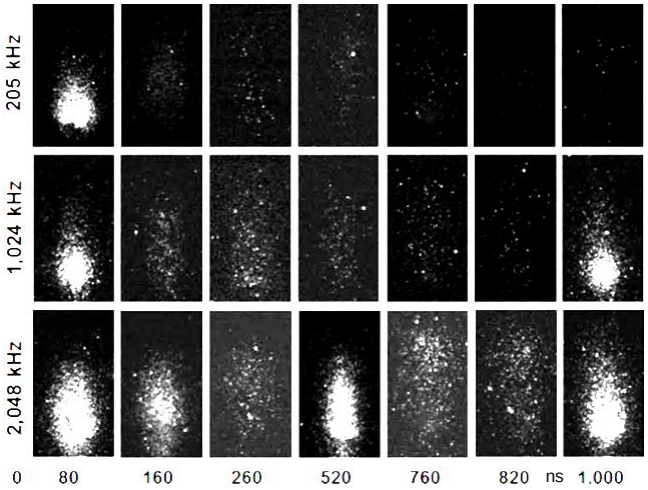

Figure 3: Ablation plumes arising on stainless steel upon femtosecond laser irradiation, pulse energy was 6 µJ; recording times after the onset of the laser pulse are given in nanoseconds**.**

3. Experimental

3.1 Laser systems

In this study two different high-PRF femtosecond laser systems were used. The *IMPULSE*^{TM} laser (Clark-MXR) supplied a maximum laser power of 13.2 W at the work piece surface, whilst the maximum laser power of the *sci-series* laser (Active Fiber Systems) was 31.7 W. The maximum laser pulse repetition rate of both systems was in the range of 20 MHz. Further, with increasing repetition rate, the maximum available single pulse energy decreased due to constant supplied maximum laser power.

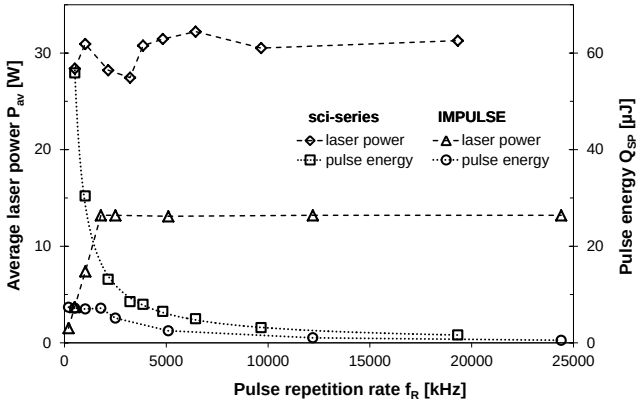

Figure 4: Average laser power and pulse energy versus repetition rate for both the *sci-series* and the *IMPULSE* ™ laser.

The proportional relation between laser power and repetition rate can be seen in Figure 4. The most important parameters of the investigated laser systems are summarized in Table 1.

Table 1: Laser parameters; *) on work piece surface.

Parameter	*IMPULSE*™ (Clark-MXR)	sci-series (Active Fiber Systems)
central wave length λ	1030 nm	1030 nm
repetition rate f_P	0.2 … 24.4 MHz	0.05 … 19.3 MHz
max. laser power*) P_{av}	13.2 W	31.7 W
max. pulse energy*) Q_P	7.2 µJ	55.9 µJ
min. pulse duration τ_H	180 fs (sech²)	350 fs (sech²)
beam propagation factor M^2	< 1.3	< 1.5

3.2 Scan systems

Two galvanometer scanner systems were utilized to deflect the laser beam across the sample surface. Compared to the *intelliSCAN 14* system, the *intelliSCANde 30* scanner provided both a considerably higher maximum scan speed and a larger scan field due to the longer focal length of the focusing objective. This is highly beneficial for prospective industrial applications of the technology due to the potentially increased processing speed, throughput, and working range. Further, strong focusing of the laser beam by the use of the *intelliSCANde 30* system produced a small focus diameter. This was little smaller than the focus diameter of 30.1 µm, achieved with the *intelliScan 14*. Galvanometer scanner parameters are given in Table 2.

Table 2: Galvanometer scanner parameters.

Parameter	*intelliSCAN 14* (Scanlab AG)	*intelliSCANde 30* (Scanlab AG)
focal length f	56 mm	163 mm
focus diameter $d_{0.86}$	30.1 µm	22.0 µm
max. scan speed v_S	4.5 m/s	17.1 m/s
max. scan field (width x length)	25 x 25 mm²	80 x 80 mm²
max. peak fluence on sample H_0	2.0 J/cm²	29.5 J/cm²

3.3 Materials and methodology

Two different materials have been investigated in this study, the black zirconium oxide ZrO_2, 94.5 %, partly Y_2O_3-stabilized (TZ-Black, Tosoh Corp.) and stainless steel X 5 CrNi 18-10 (1.4301, AISI 304). In these materials, standardized cavities have been produced by laser ablation using femtosecond laser pulses of both various pulse repetition rate and energy. Cavity dimensions were 2 x 1 mm² in length $\mathbf{l_X}$ and width $\mathbf{l_Y}$. Different cavity depths $\mathbf{l_Z}$ have been measured depending on the processing parameters.

The laser beam was deflected across the sample surface "line-by-line" by utilizing the galvanometer scan systems, schematically shown in Figure 5. In scan direction, the lateral spacing $\mathbf{d_X}$ between the overlapping laser pulses was determined by the scan speed $\mathbf{v_S}$ and the repetition rate $\mathbf{f_R}$ due to the relation $\mathbf{v_S = d_X \cdot f_R}$. The lateral distance between the laser processed lines was given by the hatch distance $\mathbf{d_Y}$. To increase the cavity depth, multiple numbers of scan passes $\mathbf{n_S}$ were irradiated.

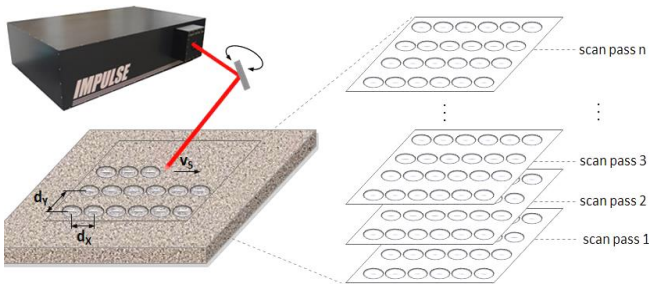

Figure 5: Schematic of the applied scan regime, were d_X is the pulse spacing, d_Y is the hatch distance, v_S is the scan speed, and n_S is the number of scan passes.

With each investigated parameter set three distinct cavities were produced. The cavity depths were measured utilizing a measurement arrangement consisting of the *Confocam C101* (confovis) and the *LV100D–U* microscope (Nikon). The measurement data were analyzed with the Mountains Map® software. The depth of each cavity was determined by eight individual depth measurements across the edge cavity, indicated in Figure 6 by the dotted line. Further, for example, the resultant depth profile is given in the lower part of the figure.

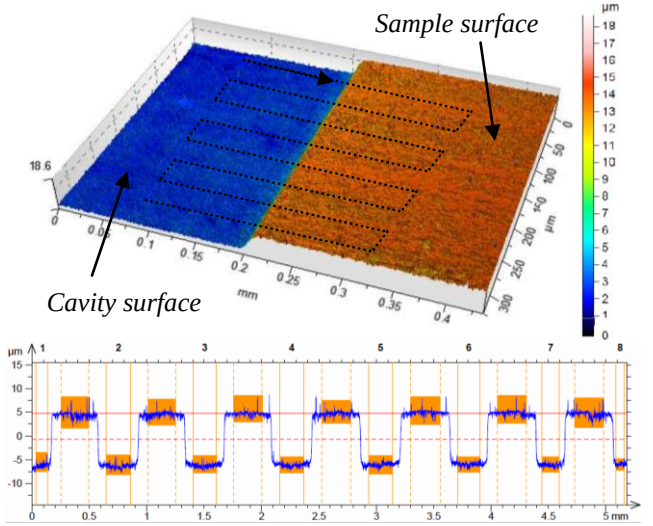

Figure 6: Laser processed cavity and depth profile.

The mean cavity depths, averaged over three cavities fabricated with constant processing parameters were used to evaluate the impact of the processing parameter on material removal. In Equation (1), the cavity depth $\mathbf{l_Z}$ is taken into calculation to determine the ablation rate $\mathbf{d_P}$. The ablation rate denotes the mean ablation depth per incident laser pulse. In this calculation, the average number of incident laser pulses per area was considered by taking into account the focus radius $\mathbf{w_0}$.

$$d_P = \frac{l_Z \cdot d_X \cdot d_Y}{n_S \cdot \pi \cdot w_0^{\,2}} \qquad \textit{Eq. (1)}$$

In addition, Equation (2) gives the volume ablation rates $\mathbf{V_P}$ as the removed material volume per irradiated laser pulse. In this equation, the laser ablated cavity volume is related to the total number of irradiated laser pulses $\mathbf{n_t}$ by taking into calculation the cavity depth.

$$V_P = \frac{V_{tot}}{n_t} = \frac{l_X \cdot l_Y \cdot l_Z}{n_t} = \frac{d_X \cdot d_Y \cdot l_Z}{n_S} \qquad \textit{Eq. (2)}$$

Finally, scaling of the volume ablation rate with the repetition rate yields the material removal rate **MRR** as the removable material volume per time.

$$\mathrm{MRR} = V_P \cdot f_R \qquad \textit{Eq. (3)}$$

4. Results and discussion

4.1 Zirconium oxide TZ-Black

Laser ablation of zirconium oxide TZ-Black was studied utilizing the *IMPULSE™* laser in combination with the *intelliSCAN 14* scan system. By using this setup, the maximum pulse energy supplied on the sample was 7.2 µm, correlating to the peak fluence of 2.0 J/cm². The pulse repetition rate and the pulse spacing were varied in the range between 20 kHz and 1.02 MHz, and 2 µm and 6 µm, respectively. The hatch distance was kept constant of 4 µm during the experiments; the number of scan passes was 25.

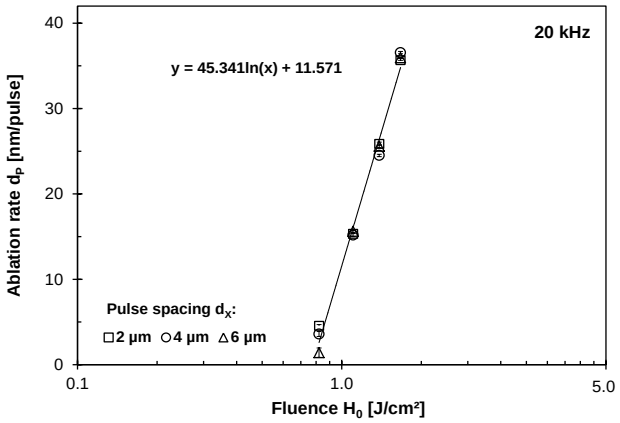

Figure 7: Ablation rate versus fluence obtained on zirconium oxide TZ-Black, the pulse spacing was varied.

Figure 7 presents the semi logarithmic plot of the ablation rate as a function of the fluence. The repetition rate was 20 kHz and the pulse spacing was varied between 2 µm and 6 µm. The ablation rate increased logarithmically with higher laser fluence and was almost unaffected by the pulse spacing. Thus, the results achieved in this processing parameter range indicate no significant impact of heat accumulation or/and particle shielding on material ablation. Further, from the regression line given in the plot, a laser energy penetration depth of 45 nm can be derived.

In addition, the volume ablation rates have been determined from the cavity depths in accordance with Equation 2, see Figure 8. The pulse spacing was constant of 4 µm. The results obtained for 20 kHz correlate closely to theoretically achieved volume ablation rates, calculated by using a method introduced in [9]. The effective penetration depth of 45 nm, given in Figure 7, and the ablation threshold of 0.48 J/cm² were used in this calculation.

Moreover, it can be seen that the ablation volume rates increase with higher pulse repetition rates. For this, heat accumulation is supposed as mainly influencing effect. It is suggested that a potential rise of the surface temperature will enhance laser beam absorption, inducing stronger material removal.

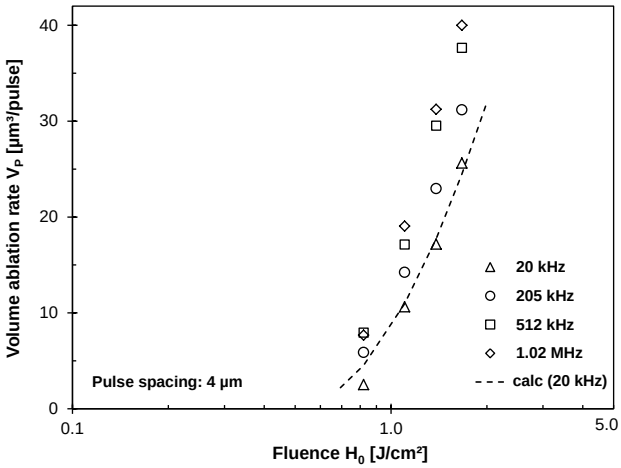

Figure 8: Volume ablation rate versus fluence obtained on zirconium oxide TZ-Black, the repetition rate was varied.

Figure 9 emphasizes the assumption that heat accumulation will enhance material removal on zirconium oxide. Volume ablation rates are given versus the pulse spacing. The pulse repetition rate and pulse energy were varied. As mentioned above, material removal by using laser pulses at 20 kHz is almost unaffected by heat, and thus no significant impact of both pulse spacing and energy on the volume ablation rate can be recognized.

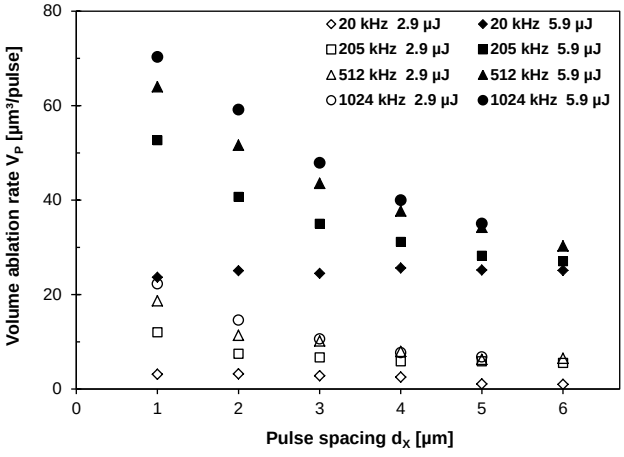

Figure 9: Volume ablation rate versus fluence obtained on zirconium oxide TZ-Black; both the pulse spacing and the repetition rate were varied.

By contrast, the ablation volume increased considerably with higher repetition rates and smaller pulse spacing. In addition, the volume ablation rates strongly enlarged with the higher pulse energy of 5.0 µJ, compared to 2.9 µJ.

The maximum achieved volume ablation rate was 70.3 µm³ per pulse, obtained with 5.9 µJ at 1.02 MHz and 1 µm pulse spacing. Scaling of this value with the repetition rate of 1.02 MHz yields the maximum possible material removal rate of 4.3 mm³ per minute. However, by using this parameter set a high thermal load of the work piece must be assumed, inducing thermal stresses. As a result, micro crack formation was observed at the bottom of the laser processed area, shown in Figure 10 (top left). The mere enlargement of the pulse spacing of 2 µm reduced the crack formation considerably, shown in Figure 10 (top right). Along with this, the maximum achievable material removal rate decreased to 3.6 mm³ per minute due to the lower thermal load.

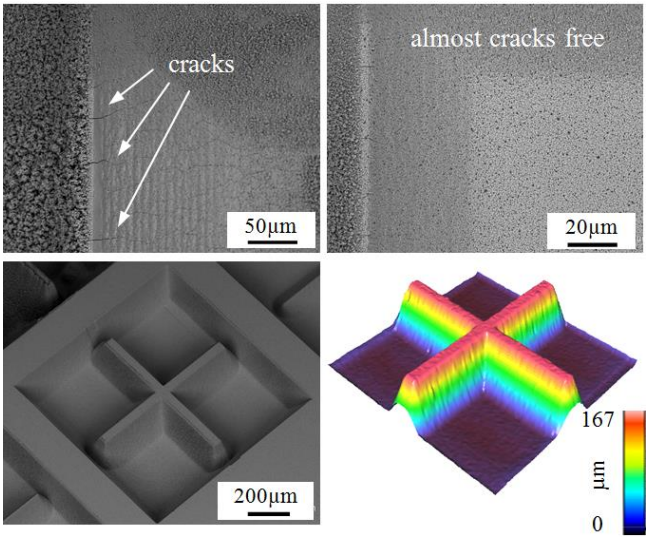

Figure 10 top: SEM images of wall edges obtained on zirconium oxide TZ-black with 5.9 µJ at 1.02 MHz and either 1 µm (left) or 2 µm (right) pulse spacing, micro cracks can be seen in the left picture; **bottom:** Demonstrator structure in zirconium oxide TZ-Black presented as SEM photograph (left) and 3D measurement (right).

The SEM photograph of a demonstrator structure made in zirconium oxide TZ-Black is presented in the lower part of the figure. Processing parameters were as follows: 5.0 µJ pulse energy, 2 µm pulse spacing, 4 µm hatch distance, and 1.02 MHz repetition rate. Structure dimension were 1 x 1 mm² in width and length. The width of the inner cross walls was 60 µm on the sample surface, and enlarged with increasing structure depth. With 25 scan passes a maximum depth of 167 µm was achieved. The processing time to fabricate this demonstrator was 19.7 seconds by applying the bidirectional scan regime.

For comparison, this demonstrator structure was processed with lowered repetition rates and thus, in turn, lowered scan speeds, whilst all other processing parameters were kept constant. By using the lower repetition rate of 205 kHz, the processing time increased to 30.5 seconds, and 160 seconds were needed at the lowest investigated repetition rate of 20 kHz. It is obvious that the processing time scales non-linearly with the repetition rates. This is the result of the applied process regime introduced in [10]. Acceleration and deceleration sections were added to the processing path to avoid pulse accumulation at the edges of the structure.

However, for the low repetition rates it was mentioned already that material removal benefitted less (or not at all) from heat accumulation. Thus, considerably smaller depths of the demonstrator were obtained with the lower repetition rates, such as 125 µm at 205 kHz, and 110 µm at 20 kHz, respectively.

4.2 Stainless steel X5CrNi 18-10 (1.4301, AISI 304)

High-PRF laser processing of stainless steel was intensively studied in our previous works within the parameter range up to 7.2 µJ pulse energy, or rather 2.0 J/cm² fluence, and 1.02 MHz pulse repetition rate by using the *IMPULSE™* laser [5-7, 10]. In these studies the increase of the ablation rate due to enhanced laser beam absorption and lowered ablation threshold initiated by heat accumulation has been demonstrated.

In this work, high-PRF laser processing of stainless steel was studied using a high laser power up 31.7 W, supplied by the *sci-series* laser. With this high laser power, the ablation threshold can be exceeded even by irradiating ultrashort pulses at high repetition rates up to 20 MHz. The laser system was used in combination with the *intelliSCANde 30*, providing much faster scan speed than the scan system used in previous experiments. The study aimed to investigate the impact of the higher laser power on both material ablation and processing speed. Another goal was the enlargement of the processing area by using a longer focus distance objective.

The maximum available laser power of 31.7 W was irradiated on the work piece surface to fabricate standardized cavities as mentioned above. The repetition rate was varied and, as a result, laser pulses at lower fluence irradiated at the higher repetition rates. The maximum laser power varied slightly with the repetition rates (see Figure 4).

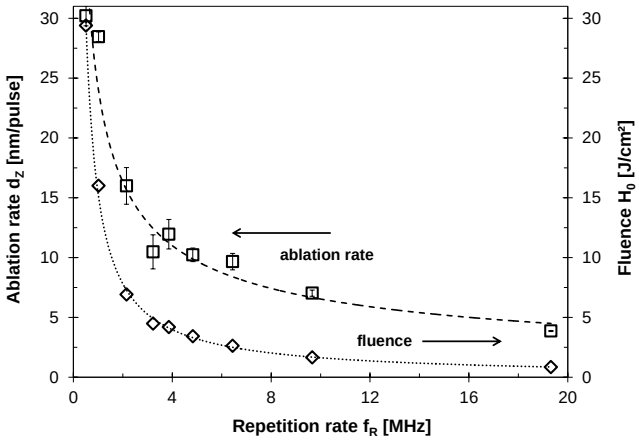

Figure 11: Ablation rate and fluence versus repetition rate obtained on stainless steel.

Figure 11 plots the ablation rate versus the repetition rate. For this, the ablation rate was calculated accordingly Equation 1 and taking into account the cavity depths obtained. Furthermore the functional dependence of the fluence on the repetition rate is presented. The maximum ablation rate of 30.2 nm / pulse was achieved with pulses of

29.4 J/cm². This was the highest investigated fluence, available at 508 kHz repetition rate. The ablation rate decreased with the higher repetition rates, mainly affected by the lower fluence.

The functional correlation between the volume ablation rate versus the repetition rate is presented in Figure 12. The plot indicates the decrease of the volume ablation rate with higher repetition rate, which is in accordance with Figure 11. Further, the material removal rate is given, calculated by scaling of the volume ablation rate with the repetition rate accordingly Equation 3. It can be seen that the material removal rate increased with the higher repetition rate, in spite of the decreasing amount of material that was removed per laser pulse. The maximum material removal rate was found to be 6.8 mm³ / min, achieved with laser pulses of 0.85 J/cm² and 19.3 MHz.

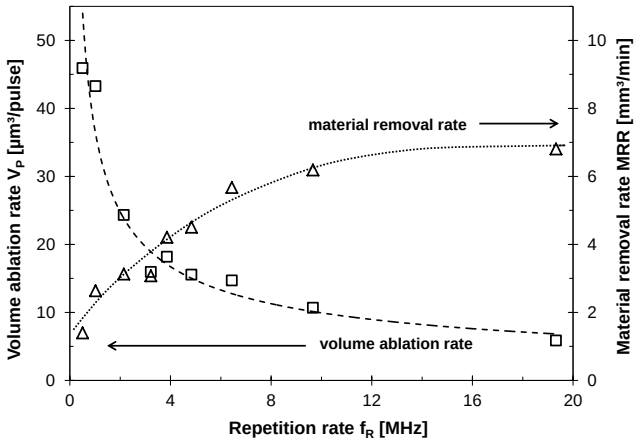

Figure 12: Volume ablation rate and material removal rate versus repetition rate obtained on stainless steel.

However, this fluence available at the highest repetition rate is almost eight times above the ablation threshold of stainless steel, which was $H_{th} = 0.1$ J/cm². According to this, it is noteworthy that the highest ablation efficiency was reported for laser pulses of a fluence about 7.4 times higher the ablation threshold [11].

SEM photographs of laser processed cavity surfaces obtained with different fluence are summarized in Figure 13. In all cases, almost the same laser power was irradiated. The fluence decreased depending on the increase of the pulse repetition rate. It can be seen that the surface quality was strongly influenced by the processing parameters.

The best machining quality was reached with the lowest fluence of 0.85 J/cm² and the highest repetition rate of 19.3 MHz. The laser processed surface appeared smooth without any micro craters, and neither re-deposited ablation products (debris) nor molten bulges can be seen. Further, a minor heat load of the work piece can be suggested in spite of the high irradiated laser power. This might be due the low fluence of the irradiated laser pulses and the high processing speed.

Furthermore, in the figure it can be seen that laser processing with laser pulses of higher fluence at the lower repetition rates caused rough surfaces. The cavity bottoms were littered with micro craters, re-deposited ablation products, as well as molten and re-solidified fragments. By contrast, high-regular and smooth cavity surfaces have been further achieved with the highest irradiated fluence of 29.4 J/cm² at the lowest repetition rate of 508 kHz. However, a number of deep micro craters appeared randomly at the laser processed surface.

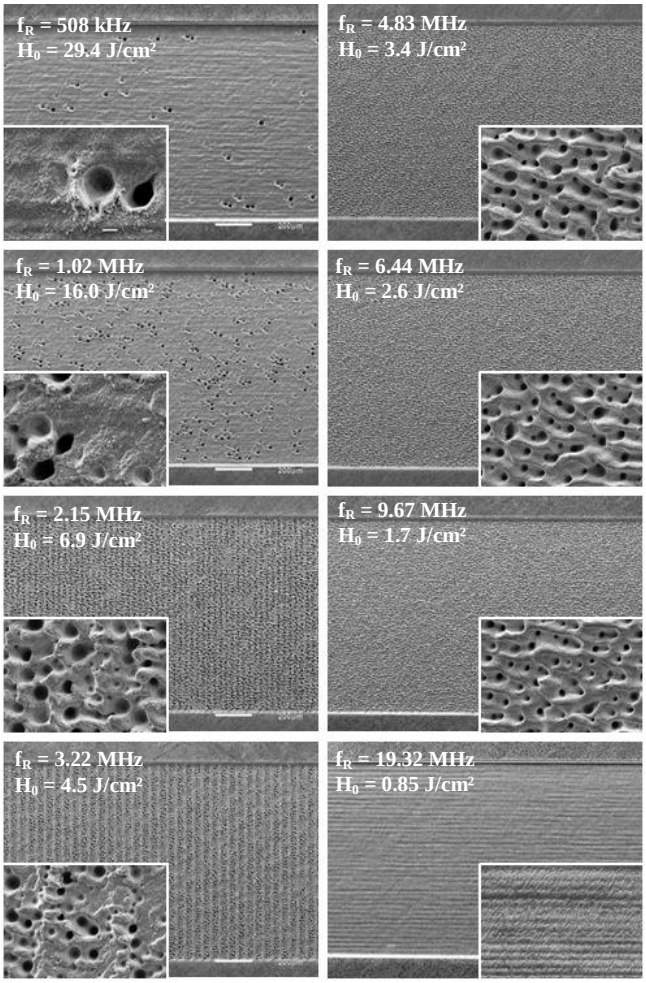

Figure 13: SEM photographs of laser processed cavity surfaces obtained with increasing repetition rates and decreasing fluence, respectively; cavity width was 1 mm.

Figure 14 presents white light illumination of a rectangular diffraction pattern, laser processed on stainless steel with the dimension of 80 x 80 mm² in width and length. Ripple formation can be recognized in the small picture.

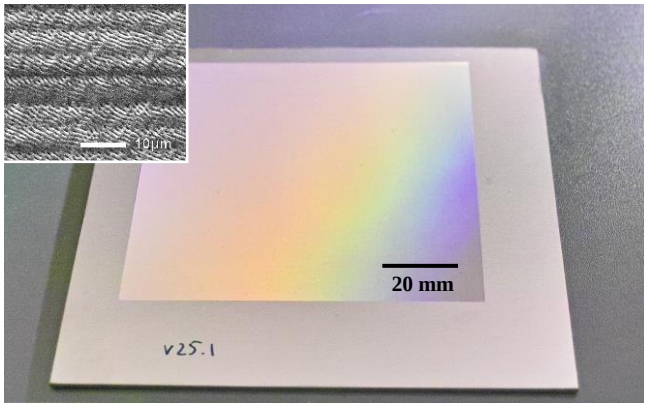

Figure 14: Rectangular diffraction pattern of 80 x 80 mm² (width x length) achieved on stainless steel, processing parameters were: 1.0 J/cm² fluence, 3.2 MHz repetition rate, 11.3 m/s scan speed, 5 µm hatch distance and 1 scan pass.

This demonstrator was fabricated with laser pulses of 1.0 J/cm² and 3.2 MHz repetition rate. The pulse spacing was 3.5 µm and the scan speed 11.3 m/s, respectively. The hatch distance was 5 µm and acceleration / deceleration sections were applied. The processing time for one laser pass in total was 157 seconds. As a result, a processing rate of 25 cm²/min was achieved. This is about three times faster than processing rates demonstrated before by utilizing the *intelliSCAN 14* system. The processing area of this scanner configuration was smaller than 25 x 25 mm² with a maximum processing rate of about 8 cm²/min.

Summary

High speed laser processing of zirconium oxide TZ-Black and stainless steel was studied. Two different high-PRF femtosecond laser systems were utilized in combination with fast galvanometer scanner systems.

Zirconium oxide TZ-Black was irradiated with a maximum laser power of 7.2 W. The pulse energy, the repetition rate and the pulse spacing were varied. A significant impact of heat on material removal was identified. The maximum achieved volume ablation rate was 70.3 µm³ per pulse, obtained with 5.9 µJ at 1.02 MHz and 1 µm pulse spacing. Scaling of this value with the repetition rate of 1.02 MHz yields the maximum material removal rate of 4.3 mm³ per minute. By irradiating laser pulses with this small spacing of 1 µm, crack formation was observed on the walls of a micro-featured demonstrator. This might be caused by thermal stresses.

The maximum available average laser power of 31.7 W was irradiated on stainless steel. The repetition rate was varied, inducing the decrease of the applied fluence. The maximum ablation rate of 30.2 nm / pulse was achieved with pulses of 29.4 J/cm² at 508 kHz. The maximum material removal rate of 6.8 mm³ / min, by contrast, was achieved with laser pulses of 0.85 J/cm² and 19.3 MHz. The high processing speed was demonstrated by means of a diffraction pattern. This rectangular structure of 80 x 80 mm² was processed with a rate of 25 cm²/min.

Acknowledgments

The presented results have been conducted in the course of the projects ”Innoprofile Transfer – Rapid Micro/Hochrate-Laserbearbeitung” (03IPT506X), funded by the Federal Ministry of Education and Research, “Fabrication and investigations of spintronic layer systems – Spintronic”(60714/226), funded by the European Union (European Regional Development Fund – EFRE) and the Free State of Saxony, Germany, and the CLUSTER project “Gecko TP-V Reibwerterhöhende Laserstrukturierung" (AiF 17228 BR/1), funded by the Federal Ministry of Economics and Technology. Further the authors gratefully acknowledge Felix Dreisow for his assistance in using the *sci-series* laser.

References

[1] Ancona, A., et al.: *High speed laser drilling of metals using a high repetition rate, high average power ultrafast fiber CPA system,* Opt. Express, 2008. **16**(12): p. 8958-8968.

[2] Döring, S., et al.: *Microdrilling of metals using femtosecond laser pulses and high average powers at 515 nm and 1030 nm.* Applied Physics A: Materials Science & Processing, 2010. **100**(1): p. 53-56.

[3] Nolte, S., et al.: *High Repetition Rate Ultrashort Pulse Micromachining with Fiber Lasers*, Fiber Laser Applications, 2011, Optical Society of America.

[4] Tan, B., S. Panchatsharam, and K. Venkata Krishnan: *High repetition rate femtosecond laser forming sub-10 µm diameter interconnection vias*, Journal of Physics D: Applied Physics, 2009. **42**(6): p. 065102.

[5] Schille, J., et al.: *Micro structuring with highly repetitive ultrashort laser pulses*, LPM2008 - 9th Symp. on Laser Precision Micromachining, Quebec (Canada), 2008.

[6] Schille, J., et al.: *Micro processing of metals using a high repetition rate femtosecond laser: from laser process parameter study to machining examples*, Proc. of 30th Int. Congress on Appl. of Lasers and Electro-Optics, Orlando (USA), paper #M102, 2011.

[7] Schille, J., et al.: *Characterisation of interaction phenomena in high repetition rate femtosecond laser ablation of metals*, Proc. of 31th Int. Congress on Appl. of Lasers and Electro-Optics, Anaheim (USA), p. 949 – 958, 2012.

[8] D. V. Tran, et al.: *Direct observation of the tempera ture field during ablation of materials by multiple femtosecond laser pulses*, Applied Surface Science, Vol. 253, no. 17, 2007, pp. 7290-4.

[9] Neuenschwander, B., et al.: *Processing of metals and dielectric materials with ps-laserpulses: results, strategies, limitations and needs*, Laser Applications in Microelectronic and Optoelectronic Manufacturing XV, San Francisco (USA), 2010.

[10] Schille, J., et al.: *An ultrafast femtosecond fibre laser as a new tool in Rapid Microtooling*, Proc. of LAMP 2009 - the 5th Int. Congress on Laser Advanced Materials Processing, Kobe (Japan), ThOL 1-3 (#151), 2009.

[11] Raciukaitis, G., et al.: *Use of High Repetition Rate and High Power Lasers in Microfabrication: How to Keep the Efficiency High?* LPM2008 - 9th Symp. on Laser Precision Micromachining, Quebec (Canada), 2008.